The International Journal of Advanced Manufacturing Technology (2024) 130:4699–4712
https://doi.org/10.1007/s00170-024-13035-7

ORIGINAL ARTICLE

Effect of nozzle wear on mechanical properties of 3D printed carbon fiber-reinforced polymer parts by material extrusion

Iacopo Bianchi[1] · Tommaso Mancia[1] · Chiara Mignanelli[1] · Michela Simoncini[1]

Received: 2 October 2023 / Accepted: 13 January 2024 / Published online: 19 January 2024

Abstract

A widespread problem of manufacturing processes is represented by the occurrence of tool wear that can lead to both poor surface finish and poor mechanical properties in the workpiece. This issue affects also additive manufacturing technologies such as the material extrusion technique. In this process, the wear mechanisms of the extrusion nozzle can be severe, in particular when materials with a high abrasive capacity, such as carbon fiber-reinforced polymers, are 3D printed. Despite the significance of this problem, scientific literature lacks systematic evaluations of nozzle wear and its correlation with parts mechanical properties. In this framework, the present paper aims at investigating the effect of the nozzle wear evolution on the mechanical properties of additively manufactured parts in short carbon fiber-reinforced polyamide. To this purpose, 3D printing processes were performed. The time dependence of the nozzle wear was analyzed by interrupting the additive manufacturing process at fixed time intervals. To analyze the effect of nozzle wear on the mechanical performances of printed parts, tensile specimens were 3D printed and tested at room temperature. A reduction in mechanical performances of the printed samples and a worsening in the surface quality were observed with increasing the nozzle wear. Optical microscopy investigation and X-ray computed tomography were used to monitor the external and internal nozzle wear evolution. The surface roughness measurements were performed to evaluate the surface quality of the 3D printed parts. Furthermore, the scanning electron microscopy was used to observe the three-dimensional topography of the longitudinal sections of filament in Carbon PA, at different printing time values, and fractured surfaces of tensile samples. This study can help to better understand nozzle wear and to predict tool service life for industrial applications. In addition, it can prompt future studies focused on the reduction of tool wear.

Keywords 3D printing · Carbon fiber-reinforced polymers · Tool wear

1 Introduction

In recent years, traditional subtractive manufacturing processes are frequently substituted by additive manufacturing (AM) technologies, which represent one of the main advances in the fourth industrial revolution. These manufacturing techniques were developed in the last decades and are continuously growing and becoming progressively relevant for 3D part production [1, 2]. These processes allow manufacturing components using an approach consisting of high-precision layer by layer material deposition. Thus, it is possible to add material only where it is necessary, avoiding the typical wastes of material of subtractive technologies. This purpose can be achieved through the topology optimization method that leads to both minimize the amount and spatially optimize the distribution of material within a given domain, while maintaining their mechanical strength [3]. Furthermore, additive manufacturing techniques enable to realize components using new and smart materials, to obtain complex shapes and low tolerances, which cannot be obtained by traditional processes [4]. In this way, there is a significant increase in the design and manufacturing freedom. AM provides many advantages, such as the possibility to produce optimized structural geometries also using mixed materials and to reduce manufacturing costs, carbon dioxide emissions, and energy demand over product's lifespan, resulting in noteworthy environmental benefits [4, 5]. Additive manufacturing processes are widespread in many

✉ Iacopo Bianchi
i.bianchi@pm.univpm.it

[1] Department of Industrial Engineering and Mathematical Science, Università Politecnica delle Marche, Via Brecce Bianche 12, Ancona, Italy

engineering fields such as bioengineering [6] and maritime [7] fields, structural engineering [8], and in automotive and aerospace sectors [9]. Recent advancements in the additive manufacturing enable the use of these technologies also to produce composite materials components as shown in [10], in which fused filament fabrication (FFF) process was used to successfully manufacture isogrid components in short carbon fiber-reinforced polymer (CFRP) composite. FFF is one of the most common AM processes which allows the use of this kind of materials. Several studies concerning FFF process of both polymer and composite materials are available in scientific literature; they are mainly focused on the investigation of the effect of process parameters on both mechanical properties and quality of printed components and their optimization [11–18].

A widespread problem in the industrial applications is related to the tool wear, that is the progressive change in the tool shape from its original shape during manufacturing processes. As far as the conventional manufacturing processes, such as computerized numerical control (CNC) machining of composite and metallic components or plastic injection molding process, are concerned [19, 20], many studies aimed at evaluating the tool wear evolution and its effect on the mechanical properties of the produced parts [19–22]. Severe mold surface wear was registered in injection molding processes, specifically when reinforced plastics were employed as raw material, and both erosion and abrasion phenomena can be observed [21, 22]. Also in FFF process, the occurrence of the nozzle wear during 3D printing process, caused by the material flow during extrusion operation, can be a relevant problem since some drawbacks can arise, such as the excessive surface roughness of the workpiece, the reduction of the nozzle accuracy during the filament deposition, the decrease in tool life, and the wrong dimension of the filament diameter during printing operation. Olsson et al. observed such phenomena during FFF process of highly abrasive materials [23]. However, no accurate evaluation of nozzle wear and its correlation with the mechanical properties of printed parts were included in their study. In fact, despite the relevance of this issue, scientific literature lacks research focused on nozzle wear mechanisms and their effects on the quality and performances of the produced components. In this context, a complete understanding of the effects of the tool wear on the mechanical properties of the produced parts becomes compelling to guarantee compliance with the design requirements; moreover, a systematic evaluation of the nozzle wear could help to increase its service life, with consequent benefits in terms of cost and environmental sustainability.

The present paper aims at studying the effect of the nozzle wear on the mechanical properties of 3D printed parts in Carbon PA by means of FFF process, identifying the correlation between the nozzle wear and the mechanical performances of the material, with relevant and immediate industrial effects. By interrupting the additive manufacturing process at fixed time intervals, the time dependence of the nozzle wear was investigated. The mechanical properties of printed parts were evaluated as a function of toll wear by means of tensile tests. Furthermore, both the external and internal nozzle wear evolution and the surface quality of the 3D printed parts were monitored by means of optical microscopy investigation and X-ray computed tomography.

The present work is organized as follows: after the Introduction, Section 2 describes the material and experimental procedures used to manufacture the printed parts, characterize their mechanical properties, and to evaluate the nozzle wear evolution as a function of printing time. Section 3 is focused on the discussion of results. Finally, conclusions are briefly reported in Section 4.

2 Materials and experimental procedures

2.1 Material

The material investigated in the present paper is a Polyamide 6 matrix reinforced with 20% in weight of short carbon fibers (up to 250 µm in length) named Carbon PA, supplied in form of filament with a diameter of about 1.75 mm [4]. The main mechanical properties of Carbon PA, provided by the supplier, are summarized in Table 1.

Figure 1 shows the SEM image of cross section of filament in Carbon PA before 3D printing. It can be observed a high number of fibers randomly dispersed in the polymeric matrix, however aligned in the longitudinal direction as a result of the extrusion operation carried out for the filament production. Furthermore, a huge quantity of both micro-voids, due to the fiber pullout, and macro-voids can be observed in the Carbon PA filament. However, Bianchi et al. [24] demonstrated that these voids are significantly reduced during the 3D printing due to the decrease of filaments diameter from 1.75 to 0.4 mm.

According to the material datasheet, Carbon PA is characterized by low weight (density of 1.07 ± 0.05 kg/cm^3) and similar mechanical strength value to that obtained by aluminum alloys, making it suitable for metal replacement applications such as in automotive, aerospace, and military industries [25, 26]. However, the presence of highly abrasive

Table 1 Main tensile properties of Carbon PA

Carbon PA tensile properties	Value
Ultimate tensile strength [MPa]	138
Tensile modulus of elasticity [GPa]	14.7
Elongation	1.71%

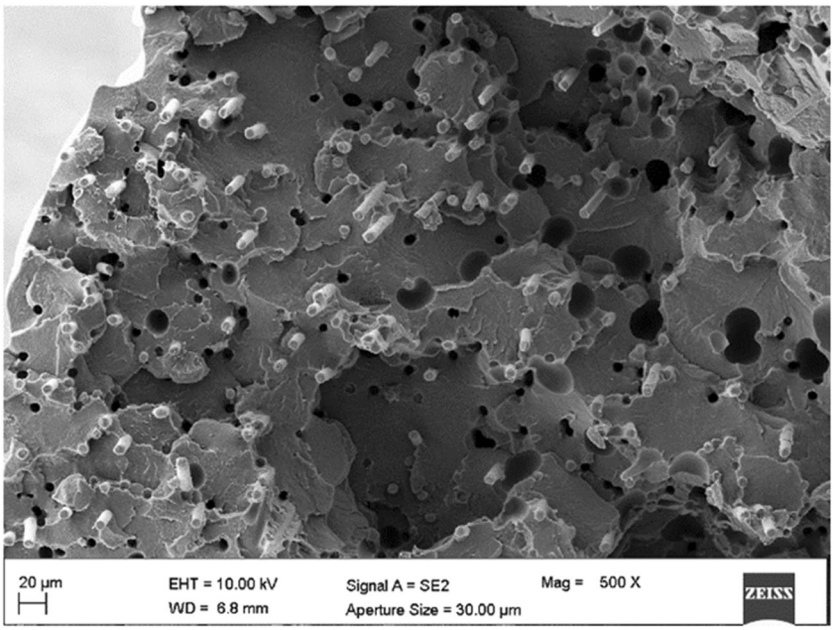

Fig. 1 SEM image of the cross section of filament in Carbon PA before 3D printing

short carbon fibers can cause wear mechanisms in the tools during processes on workpieces in Carbon PA, as reported in scientific literature [27, 28].

2.2 Experimental procedures

Figure 2 shows the schematic representation of the experimental procedures performed in the present research. Specifically, in order to investigate the influence of the nozzle wear evolution on the mechanical properties of additively manufactured components in Carbon PA, 3D printing processes were performed. The processes were interrupted at fixed time intervals to investigate the time dependence of the nozzle wear. 3D printed tensile specimens, obtained after different printing times, were tested to evaluate the mechanical properties. Finally, the external and internal nozzle wear evolution and the surface quality of the 3D printed parts, at different printing times and, consequently, at different nozzle wear levels, were monitored by means of optical microscopy investigation and X-ray computed

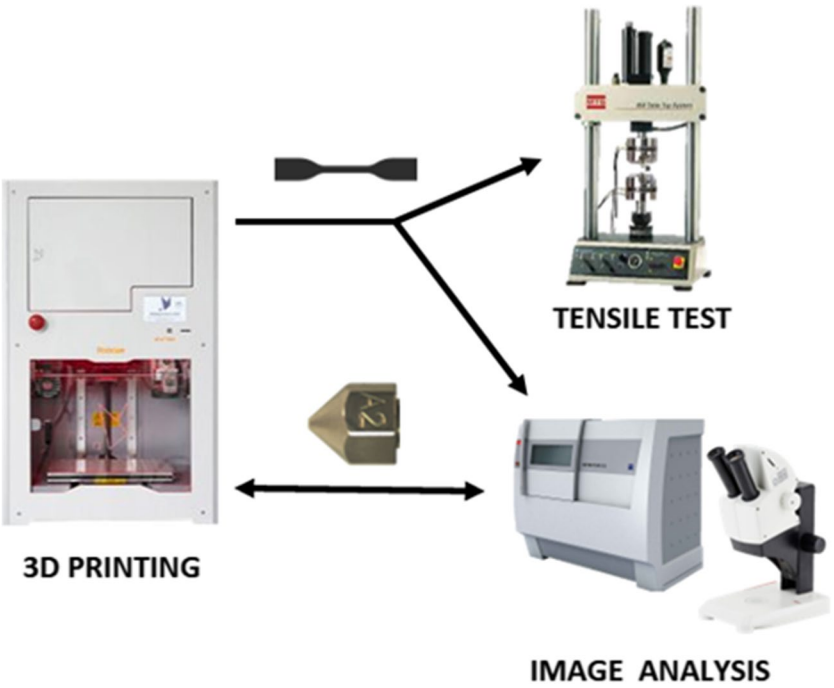

Fig. 2 Schematic representation of the followed experimental procedures

tomography. Further details on the experimental procedures are reported in the following subsections.

2.2.1 3D printing process

For the additive manufacturing process, the Roboze One+400 3D printer, equipped with FFF technology and supplied by Roboze Spa, was used to obtain components in Carbon PA. A commercial Micro Swiss MK8 nozzle with 0.4-mm extrusion diameter, realized in brass as base material and coated with a low friction nickel layer, was used during FFF operations since, according to the manufacturer datasheet, it is suitable for printing highly abrasive materials such as fiber-reinforced filaments.

The component geometry was designed using the commercial CAD software Rhinoceros. The CAD file was imported in a slicing software to set up printing parameters.

Before each printing, the filament spool was dried at 110 °C for 2 h to remove the moisture content; as a matter of fact, according to the results exhibited by [29], polyamide is strongly subjected to moisture absorption from the environment, with consequent reduction in the mechanical properties. For the same reason, during the printing process, the spool of filament in Carbon PA was kept in a dryer at a controlled temperature of 70 °C. The nozzle and the printing bed temperatures were set to 260 °C and 80 °C, respectively. A nominal printing speed equal to 50 mm/s was kept constant.

The printed parts were obtained with a complete infill (100%) and with a linear infill pattern along the tensile axis of the specimens to maximize the mechanical performances. A layer thickness equal to 0.18 mm was set.

Table 2 reports the main printing parameters. These parameters were maintained constant throughout the whole study.

The FFF process was periodically interrupted to evaluate the nozzle wear evolution as a function of printing time (t), from 0 to 5540 min. A specimen was printed using the wear-free nozzle ($t = 0$ min), so that its surface finish and mechanical performance could be compared with those obtained from specimens printed with the worn nozzle.

Table 2 Printing parameters imposed in the present investigation

Nozzle diameter	0.4 mm
Infill density	100%
Extruder temperature	260 °C
Bed temperature	80 °C
Layer thickness	0.18 mm
Average printing speed	50 mm/s

2.2.2 Tensile test

The mechanical properties of 3D printed Carbon PA composite were investigated by exploiting uniaxial tensile tests, carried out on 3D printed tensile samples with dimensions in accordance with the ASTM D638 international standard (gauge length 80 mm, thickness 4 mm, and width 10 mm), using the servo-hydraulic MTS 810 testing machine. Samples, obtained in the flat orientation coincident with print bed, were printed at different fixed time values in order to evaluate the effect of the nozzle wear on both surface finish and mechanical properties of the printed parts.

Tensile specimens were characterized by a gauge length, width, and thickness equal to 80 mm, 10 mm, and 4.5 mm, respectively. In order to prevent failure caused by the high clamping forced applied by the gripping mechanism, the grip section was increased both in thickness (6 mm) and width (20 mm). The crosshead speed was kept constant and equal to 2 mm/min.

Strength vs. displacement data were registered by means of a load cell and a Linear Variable Differential Transducers (LVDT). Moreover, a clip-on uniaxial extensometer was employed to accurately register the strain before fracture. Tensile stress vs. tensile strain curves were obtained, and the ultimate tensile strength (UTS), elasticity modulus (E), and strain to failure (ε_f) were calculated.

2.2.3 Nozzle wear evaluation

In order to monitor the nozzle wear as a function of the printing time, the image analysis system LASEZ (Leica Application Suite), which processes high-resolution and high-contrast images acquired by means of the stereomicroscope Leica EZ template 4D, was used. This instrument features a digital camera that allows to export the images and to adjust them in terms of sharpness, brightness, contrast, etc.

The geometry of the wear-free nozzle, at $t = 0$ min, is shown in Fig. 3, in which the longitudinal section cut of the nozzle can be observed. Specifically, three different diameters can be measured: the orifice diameter of the nozzle, i.e., internal diameter of the nozzle (D_i), through which the Carbon PA filament is extruded, the nozzle bore chamfered (D_o), and the external diameter of the nozzle (D_e) that delimits the tip area. In the wear-free nozzle at $t = 0$ min, $D_{i\,(t=0)} = 0.40$ mm, $D_{o\,(t=0)} = 0.51$ mm, and $D_{e\,(t=0)} = 0.87$ mm.

In order to assess the nozzle performance, a quantitative evaluation of nozzle wear was carried out. The variations of the D_i, D_o, and D_e values in percentage, equal to ΔD_i [%], ΔD_o [%], and ΔD_e [%], respectively, measured by the frontal images of the nozzle after different printing times, were used as indicators of nozzle wear and employed to evaluate the time dependence of the wear caused by the abrasion of the short carbon fibers dispersed into the filament:

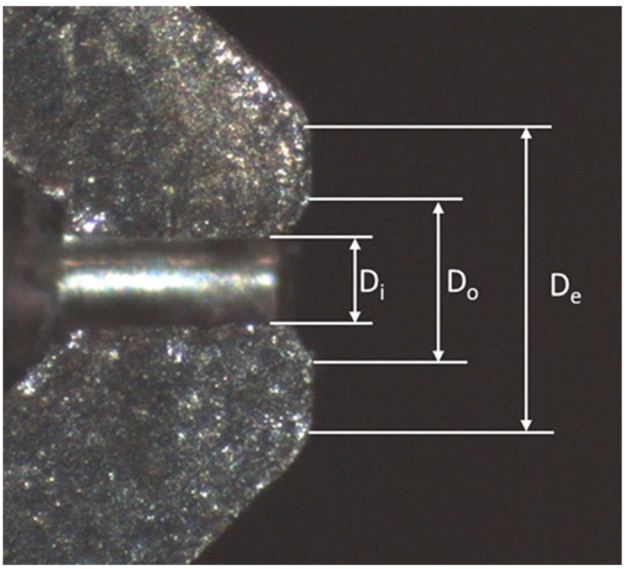

Fig. 3 Cut of the wear-free nozzle longitudinal section

$$\Delta D_i[\%] = \frac{D_{i\,(t)} - D_{i\,(t=0)}}{D_{i\,(t=0)}} \bullet 100 \quad (1)$$

$$\Delta D_o[\%] = \frac{D_{o\,(t)} - D_{o\,(t=0)}}{D_{o\,(t=0)}} \bullet 100 \quad (2)$$

$$\Delta D_e[\%] = \frac{D_{e\,(t)} - D_{e\,(t=0)}}{D_{e\,(t=0)}} \bullet 100 \quad (3)$$

where $D_{i(t)}$, $D_{o(t)}$, and $D_{e(t)}$ are the values of D_i, D_o, and D_e measured at a fixed printing time t [min].

Each measurement was repeated three times, and the average value was calculated to ensure accuracy and repeatability. The nozzle wear was detected by superimposing the image of wear-free nozzle with that of the worn one, obtained using the image processing program "ImageJ".

Furthermore, the nozzle used in 3D printing was also subjected to X-ray computed tomography (X-CT) analysis to provide high magnification images of the external and internal surfaces of the nozzle at different printing times, both in the wear-free and worn conditions, to accurately identify the tool wear mechanisms operating during FFF process of Carbon PA. To this purpose, the Zeiss METROTOM 1500 was employed to perform the X-CT analysis; the nozzle was placed vertically within the machine chamber between the X-ray source and detector systems to acquire images throughout the whole thickness of the printing tool. Table 3 summarizes the parameters imposed for the acquisition of the nozzle images by the X-CT analysis.

Table 3 X-CT machine parameters for the acquisition of nozzle images

Parameters	Value
Voltage [kV]	200
Current [μA]	72
Integration time [ms]	666
Gain	8
Voxel size [μm]	13.23
Spot size [μm]	14
Magnification	15.12

2.2.4 Surface finish of the printed parts

The effect of the nozzle wear on the surface finish of the printed parts was evaluated by acquiring high-resolution and high-contrast images of the specimen surfaces using the Leica EZ stereomicroscope. Furthermore, the surface roughness of 3D printed samples, defined through the Ra value, was measured at different printing time values using the roughness tester Mahr MarSurf PS 10.

2.2.5 Scanning electron microscope analysis

High magnifications of three-dimensional topography of the longitudinal sections of filament in Carbon PA, at different printing time values, were acquired using the scanning electron microscope (SEM) ZEISS EVO 10, equipped with energy dispersive X-ray (EDX) spectroscopy system to acquire spatially resolved elemental chemistry information. The effect of FFF technique on the short carbon fiber orientation was evaluated. Furthermore, fractured surfaces of samples subjected to tensile tests were analyzed using SEM analysis in order to obtain their high-magnification topography.

3 Results and discussion

Figure 4 shows the comparison between typical tensile specimens obtained using the FFF technology, at different printing times, before and after tensile test. No appreciable deformation in the fractured sample can be observed, denoting a brittle behavior of the composite material.

The results obtained by samples in Carbon PA printed at different printing times were plotted in terms of tensile stress versus tensile strain curves (Fig. 5). Irrespective of the printing time taken into account, the 3D printed samples are characterized by a linear elastic behavior at low strain values, with high elastic modulus which tends to decrease with increasing strain, denoting the typical behavior of the reinforced polymers [10]. Once the yield strength is reached, the stress further increases with strain until a peak value, in which the specimen failure occurs. Table 4 summarizes the

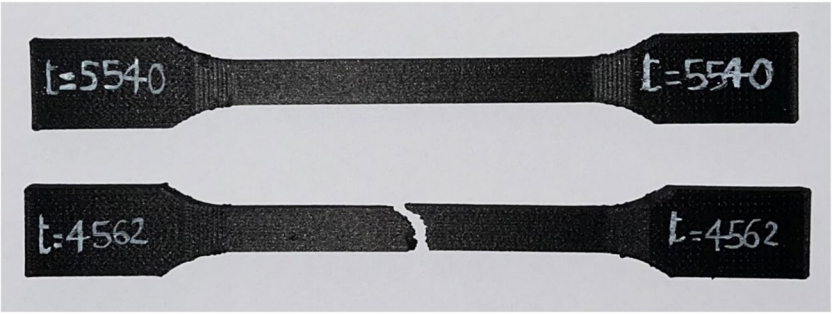

Fig. 4 Typical tensile specimens before and after tensile test

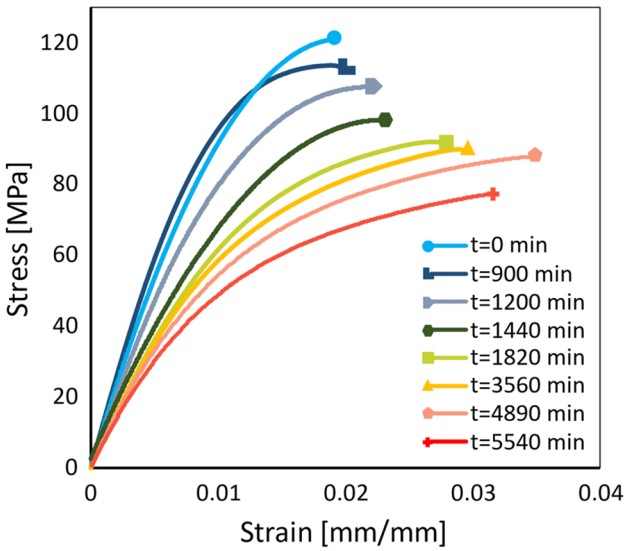

Fig. 5 Effect of printing time on typical tensile stress vs. tensile strain curves of additively manufactured specimens in Carbon PA

Table 4 Effect of the printing time on mechanical properties of specimens in Carbon PA produced using the FFF technology

t [min]	UTS [MPa]	ε_f	E [MPa]
$t = 0$	122.26	0.019	10266
$t = 100$	117.75	0.017	12784
$t = 900$	113.74	0.019	12282
$t = 1200$	107.80	0.022	9525
$T = 1440$	97.54	0.023	8212
$t = 1820$	91.98	0.027	7393
$t = 3260$	95.65	0.025	8840
$t = 3560$	89.90	0.029	7286
$t = 3920$	75.72	0.033	6051
$t = 4562$	75.98	0.035	6046
$t = 4890$	88.54	0.034	6918
$t = 5540$	76.68	0.034	6343

results of the tensile tests in terms of UTS, E, and ε_f for the specimens in Carbon PA produced using the FFF technology with different printing time values. As far as the effect of the printing time on stress-strain curves is concerned, it can be noted that, for a given strain value, the specimens printed after low printing time values exhibit strength levels higher than those obtained by specimens manufactured after high t values. Furthermore, the 3D printed samples are characterized by the increase in strain to failure values with increasing printing time. Such behavior is more marked if high printing time values are considered, as shown in Fig. 6 in which the UTS and e_f behaviors are shown as a function of time; conversely, from a t value ranged from 0 to about 1000 min, the effect of printing time on mechanical properties of 3D printed specimens is negligible. As a matter of fact, the UTS exhibited by 3D printed specimens tends to decrease of about 7% with increasing printing time from 0 to about 1000 min, while it reduces by 37% when t value further decreases up to 5540 min (Fig. 6a). Also, E value tends to decrease with rising printing time, with a marked effect when the t value increases from 900 to 5540 min (Table 4). On the other hand, as the printing time increases from 0 to 5540 min, an enhancement of the specimen ductility can be observed, with an increase in maximum strain to failure higher than 75%.

As far as the effect of the printing time on stress-strain curves is concerned, it can be noted that the mechanical behavior of the 3D printed parts is affected by t values. Specifically, from a printing time ranging from 0 to about 900 min, the effect of printing time on mechanical properties of 3D printed specimens is negligible. However, for a given strain value, the specimens printed at the low printing time values of 0 and 900 min exhibit strength levels and elastic modulus values higher than those obtained by specimens manufactured after higher printing times, even though their ductility is poor. As a matter of fact, the 3D printed samples are characterized by the increase in strain to failure values with increasing printing time. Such results can be observed in Fig. 6 that shows the UTS and e_f values as a function of time. The UTS exhibited by 3D printed specimens tends to decrease of about 7% with increasing printing time from 0 to about 900 min, while it reduces by 37% when t value further decreases up to 5540 min (Fig. 6a). Also, the E value tends to decrease with rising printing time, with a marked effect when the t value increases from 900 to 5540 min (Table 4). On the other hand, as the printing time increases from 0 to

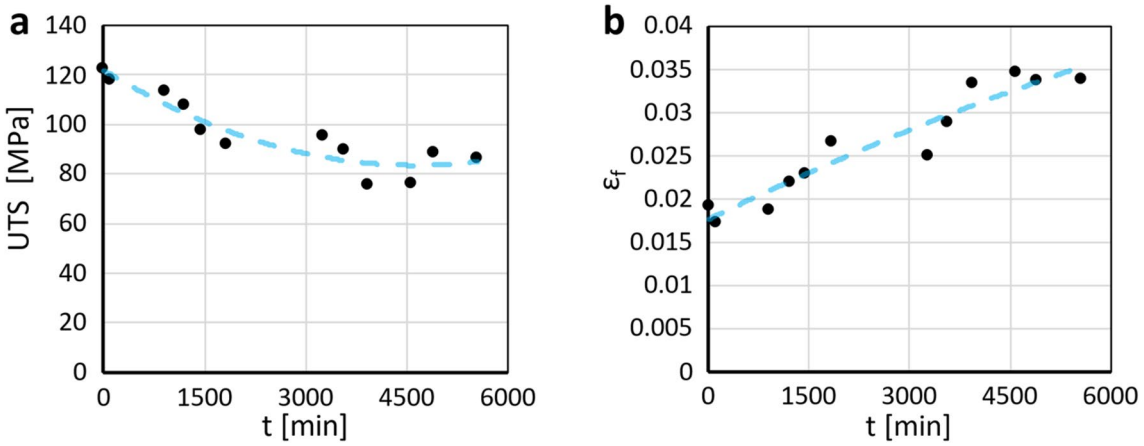

Fig. 6 **a** UTS and **b** ε_f of 3D printed specimens in Carbon PA as a function of the printing time

5540 min, an enhancement of the specimen ductility can be observed, with an increase in maximum strain to failure higher than 75% (Fig. 6b).

The variation in the mechanical properties of the 3D printed samples with the printing time can be attributed to the nozzle wear phenomena which occur during the FFF process. To this purpose, Fig. 7 shows the evolution of the nozzle external geometry acquired after interrupting FFF process at different printing times. In the wear-free nozzle condition (at $t = 0$ min), the nominal orifice diameter and the nozzle bore chamfered, marked, respectively, with the red and black circles in Fig. 7a, can clearly be observed. As the printing time increases, the wear slightly increases in the early stages of the service life of the nozzle. As shown in Fig. 7b, within the first 30 h of the printing process ($t =$ 1820 min), low wear phenomena can be noticed. As a matter of fact, both the orifice diameter and nozzle bore chamfered undergo small changes with respect to those observed for

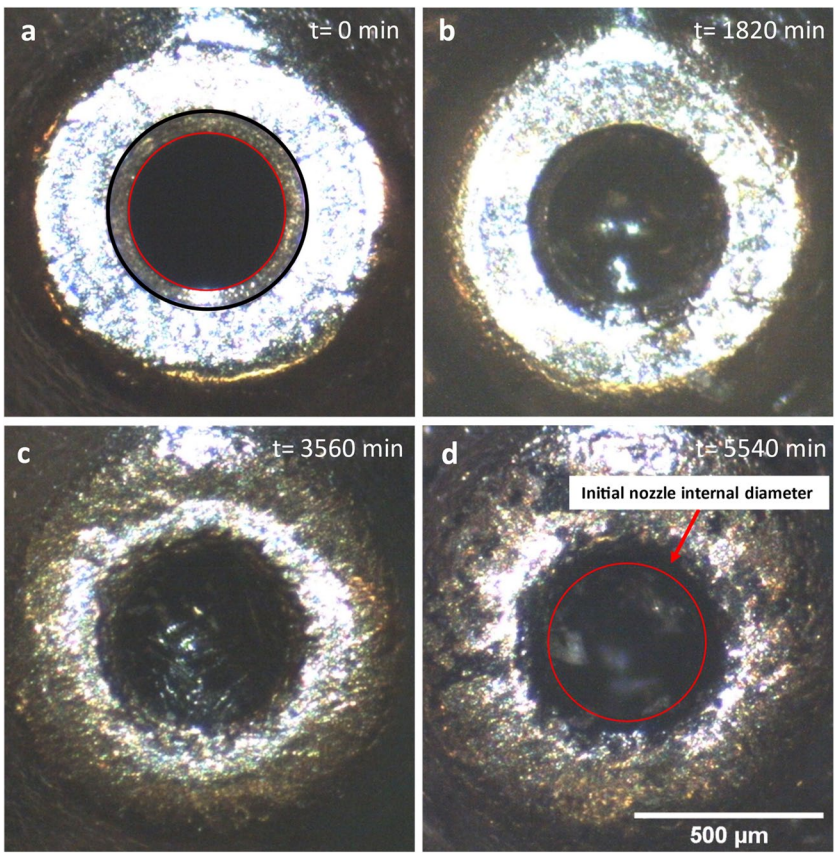

Fig. 7 High magnification of the nozzle tip area (× 35) at different printing time values: **a** 0 min, **b** 1820 min, **c** 3560 min, and **d** 5540 min

higher printing time. An initial edge rounding of the external diameter of the nozzle can be clearly seen. The nozzle tendency to progressive wear over time can be observed; as a matter of fact, as the printing time increases up to 3560 min (Fig. 7c), the nozzle exhibits severe marks of wear due to the abrasion caused by the short carbon fibers dispersed into the filament on the external nozzle surface. Specifically, the nozzle wear involves primarily the increase in the bore chamfered and the drastic edge rounding of the external diameter, leading to a serious tip area decrease; the severe rounding of the external edge does not allow monitoring the evolution of the external diameter De as a function of the printing time. The wear mechanism further tends to worsen the shape of the nozzle over time, as can be seen in Fig. 7d when the t value is equal to 5540 min.

The nozzle wear was also observed by considering the longitudinal tool side; Fig. 8a shows the longitudinal profiles of the wear-free nozzle at $t = 0$ min and of the worn one at $t = 5540$ min that were derived and overlayed by means of the analysis software ImageJ. The wear is particularly enhanced on the external surfaces of the nozzle, where abrasion phenomena occur due to the contact between the tool and the deposited extruded material (Fig. 8b). This result agrees with what reported in scientific literature about injection molding processes of fiber-reinforced plastics; as a matter of fact, the fibers tend to behave as multi-intenders transported by the molten thermoplastic material, resulting in strong tool wear [21, 22].

In order to evaluate the internal wear evolution of the nozzle during FFF process, the X-ray computed tomography analysis was performed to observe the internal longitudinal sections of the wear-free (Fig. 9a) and worn (Fig. 9b) nozzles. As it can be seen, differently from what is highlighted on the external surface of the nozzle (Fig. 7 and Fig. 8), no appreciable internal wear can be detected. In accordance with what observed in Fig. 8, also CT analysis shows the edge rounding caused by the abrasive carbon fiber of the extruded filament, located in the terminal part of the nozzle, where it is evident the almost total disappearance of the flaring that characterizes the new nozzle.

The presence of material adhered to the inner surface of nozzle can be confirmed by the reduction in section of the extruded filament using the worn nozzle (Fig. 10b) as compared to the mean value in diameter of the extruded filament obtained using the wear-free nozzle (Fig. 10a). Furthermore, the filament extruded through the worn nozzle, in addition to exhibiting many voids, poor uniformity, and a non-homogeneous section, is characterized by fibers that

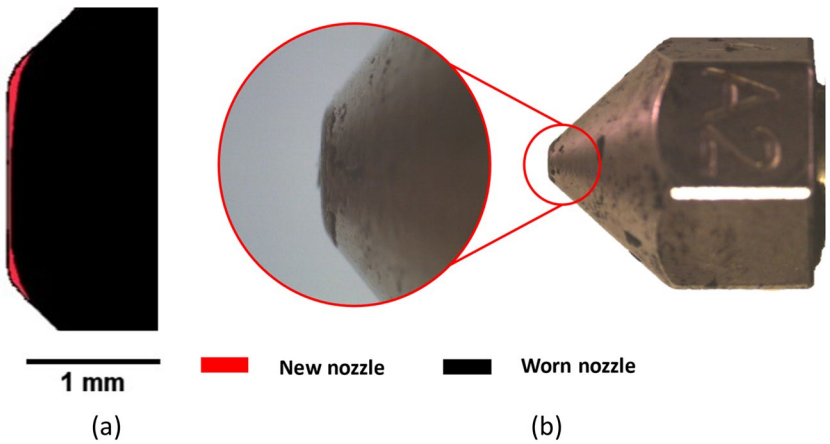

Fig. 8 **a** Superimposition between worn nozzle (at $t =$ 5540 min) and wear-free one (at $t = 0$ min) and **b** longitudinal side of the worn nozzle

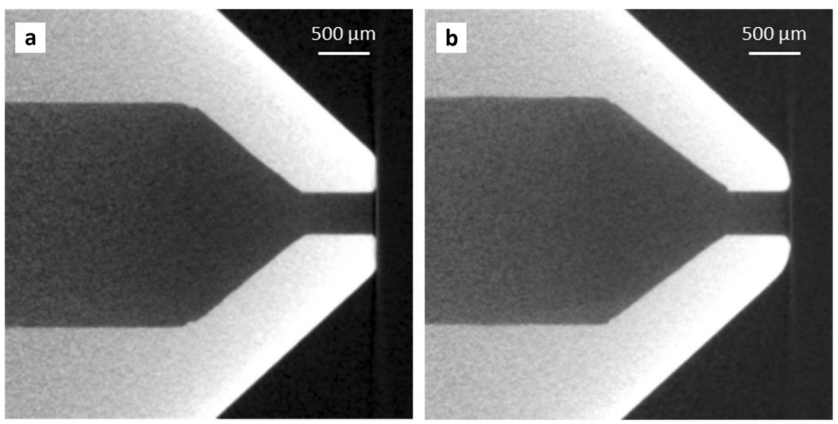

Fig. 9 X-CT section images of **a** wear-free nozzle at $t = 0$ min and **b** worn nozzle at $t = 5554$ min

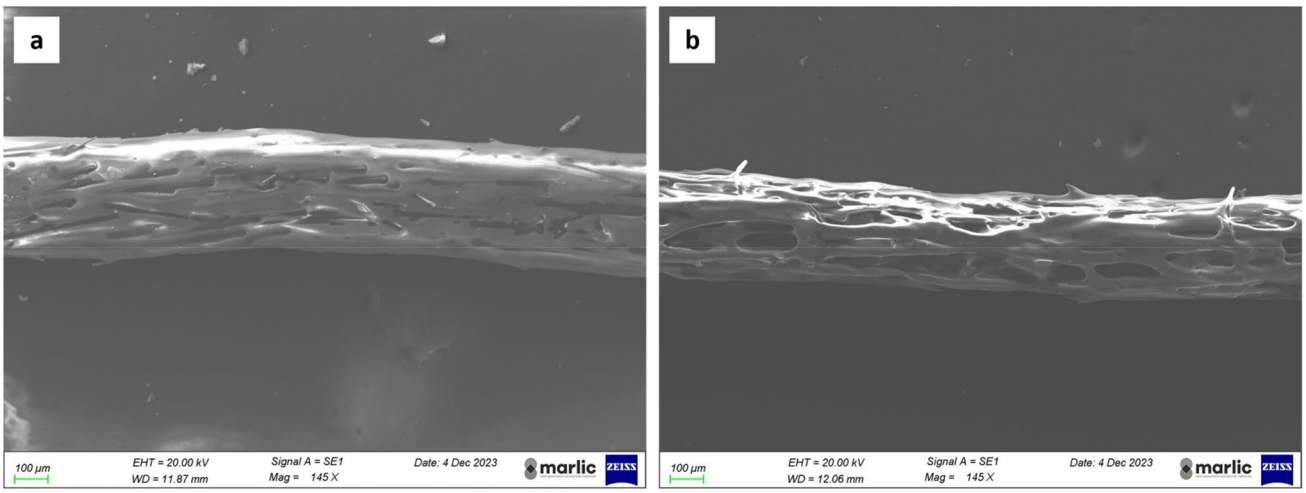

Fig. 10 High magnifications of three-dimensional topography of the longitudinal section of the extruded filament in Carbon PA using **a** wear-free nozzle (at $t = 0$ min) and **b** worn one (at $t = 5540$ min)

are not perfectly aligned in the extrusion direction, as can be seen from Fig. 10b in which some fibers protrude transversally from the filament.

Furthermore, the comparison between the X-CT section images of the wear-free nozzle at $t = 0$ min (Fig. 9a) and the worn nozzle at $t = 5554$ min (Fig. 9b) shows that the orifice diameter D_i does not undergo appreciable variations during the additive manufacturing process; for this reason, the D_i value can be considered almost constant during FFF process, that is the ΔD_i values negligible with increasing printing time.

Videos related to the tomography analysis performed on the wear-free and worn nozzles are available as additional multimedia materials (see Video 1: X-CT Free-wear nozzle and Video 2: X-CT Worn nozzle).

By considering the results shown above on the effect of the nozzle wear on the D_e and D_i values, i.e., the high difficulty in monitoring the evolution of D_e during process due to the severe rounding of the external edge and the negligible values of ΔD_i, only the behavior of ΔD_o in percentage versus printing time was analyzed (Fig. 11). As expected, ΔD_o monotonically increases with printing time, indicating that the nozzle bore chamfered strongly depends on nozzle wear. Specifically, three different phases can be observed; in the initial one, the variation of D_o rapidly increases with printing time. After a nozzle service life of about 1000 min, an increase in D_o of about 5% can be detected. The second phase, characterized by a printing time ranging from about 1000 to 3300 min, is characterized by a slight and linear increase in D_o with time. In the last phase, as printing time value further increases from about 3300 to 5540 min, the ΔD_o vs. t curve is characterized by a further increase in diameter with time, more marked as compared to the rise of ΔD_o observed in the previous phases.

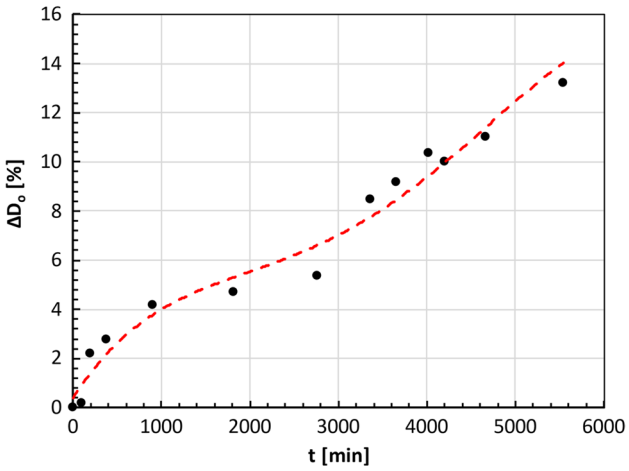

Fig. 11 Variation of D_o in percentage as a function of printing time

Since the strength and ductility of the 3D printed parts are significantly affected by the printing time, as shown in Fig. 6, the mechanical properties of such additively manufactured components in Carbon PA were related to nozzle wear. To this purpose, Fig. 12 shows that the nozzle bore chamfered variation strongly affects the UTS and e_f values. Specifically, it can be observed that the behavior of UTS and e_f are similar of those reported in Fig. 6, with a decrease in UTS and a rise in ε_f as the nozzle wear advances. Such results denote the time dependence of the nozzle wear caused by the abrasion of the short carbon fibers dispersed in the filament during the FFF process.

Furthermore, the fracture mechanism of the tensile samples in Carbon PA printed at different printing time is consistent with the time dependence of the nozzle wear. To this purpose, Fig. 13 shows the SEM images of the fracture

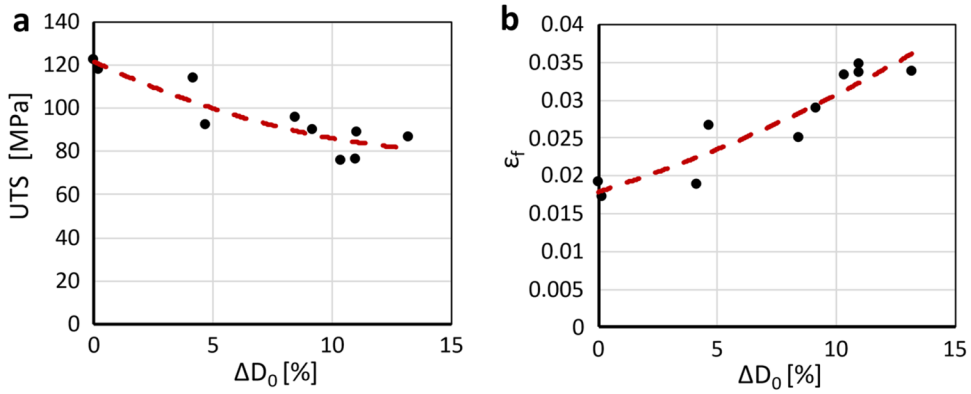

Fig. 12 UTS (**a**) and ε_f (**b**) dispersion curves in function of the variation of the outer diameter

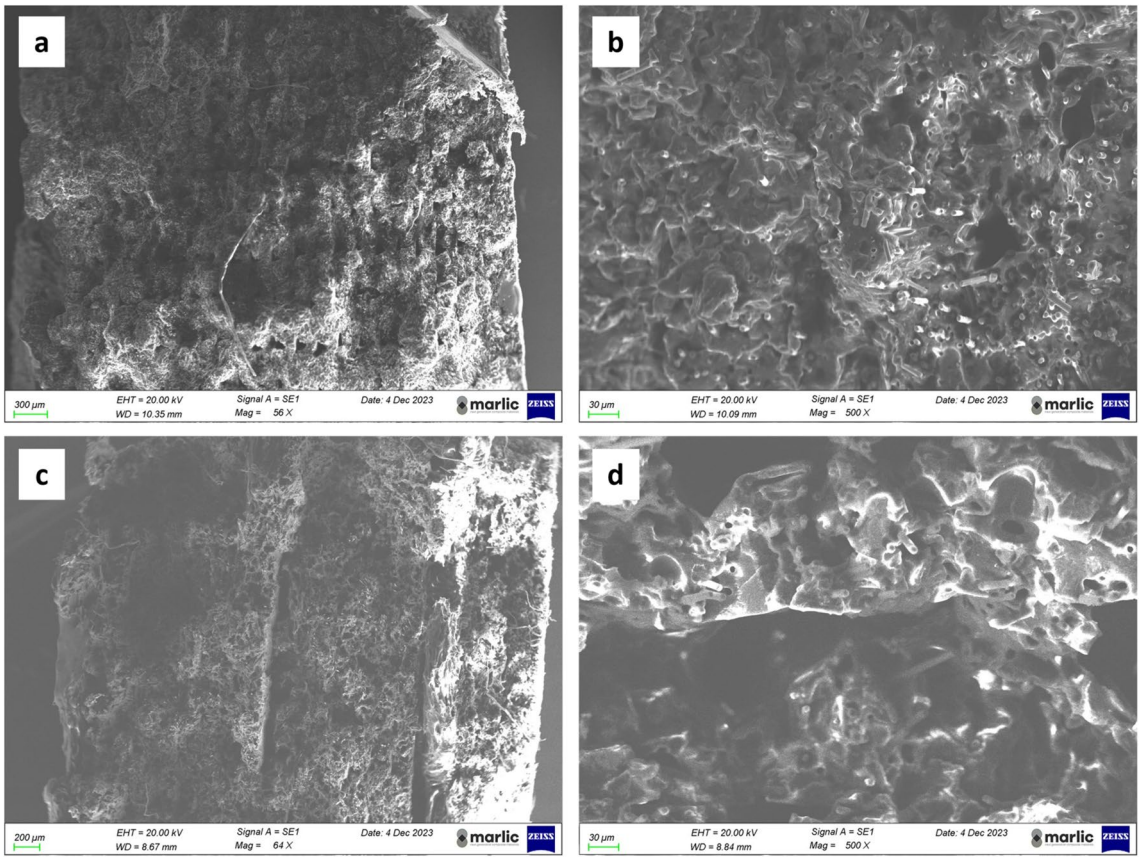

Fig. 13 Scanning electron microscopy of fractured surfaces of tensile samples printed at different printing time values: **a**, **b** $t = 100$ min; **c**, **d** $t = 5540$ min

surface of tensile samples realized at different printing time values. It can be observed that the specimen obtained at 100 min (Fig. 13a) exhibits a surface characterized by a matrix yielding and matrix and fibers debonding, due to the ductile fracture of the matrix and the physical damage of fiber-matrix interface. On the contrary, the fracture of the sample printed after 5540 min (Fig. 13b) can be attributed to the many voids and intra-layers macro defects caused by the un-uniform and non-homogeneous filaments deposited by the worn nozzle, leading to a marked reduction in tensile strength of 3D printed part at high printing time as compared to that given by the specimen printed at the initial nozzle service life.

The nozzle geometric changes, caused by the wear phenomena developed during FFF process, are responsible of the poor surface finish and the worsening of the esthetic appearance of the 3D printed parts (Fig. 14), besides that the significant variation in mechanical properties of the printed parts

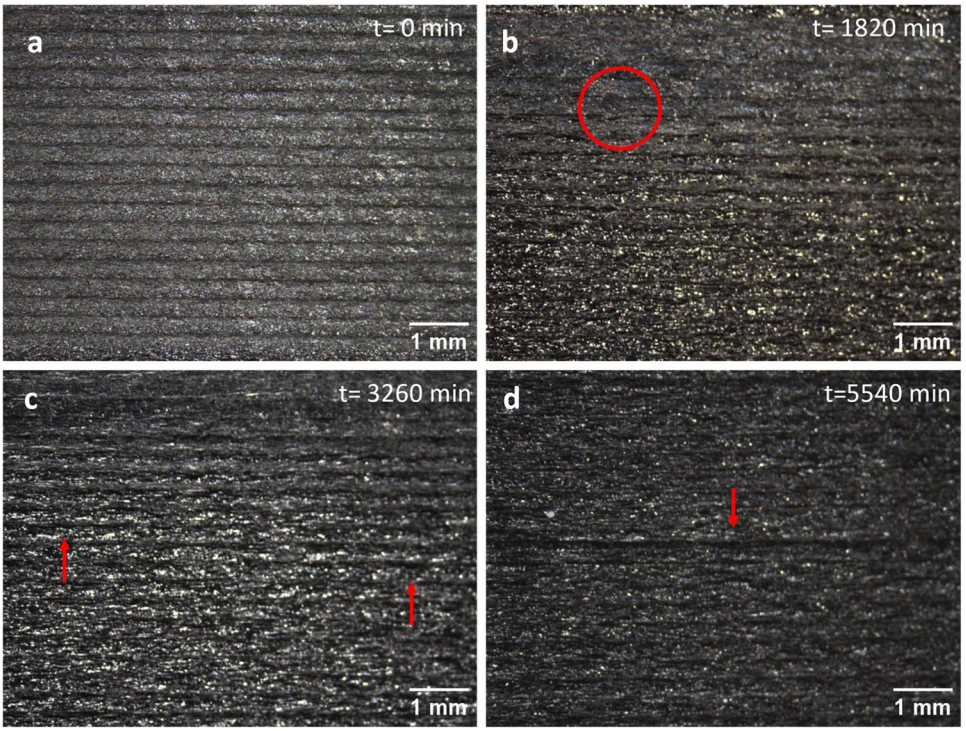

Fig. 14 Upper surfaces of 3D printed tensile specimens produced at different nozzle wear levels and detection of surface defects

(Fig. 6). In order to assess the effect of the nozzle wear on the quality of the 3D printed parts, surface images were acquired at different time values. At the initial printing time using a wear-free nozzle ($t = 0$ min), the surface of the part is characterized by a good quality, with straight printing lines with almost constant width (Fig. 14a); no macroscopic defects or porosity are visible. With increasing printing time and, consequently, nozzle wear, a progressive worsening in the surface quality appears, with high roughness, macroscopic voids and defects. After a nozzle service life of about 1820 min, the extruded filament width shows inhomogeneities, with zones characterized by increasing and decreasing filament width in the same printing line. As a matter of fact, as the service life increases, the D_o diameter increases, and the hole profile becomes less sharp, resulting in a less smooth material flow. For the same reason, voids (such as the one marked by the red circle of Fig. 14b) and macroscopic defects, highlighted by the red indicator of Fig. 14c) are widespread in the surfaces of the printed part at 3260 min. At the last printing time investigated (Fig. 14d), a macro crack can be clearly observed.

If the quality of the surface finish in terms of roughness is taken into account, from the values obtained from roughness tests, it can be seen that the surface roughness increases by approximately 10 times, going from Ra = 1.7 µm obtained for the specimen realized at $t = 0$ min up to Ra = 14.1 µm for the specimen obtained at $t = 5540$ min.

The results in terms of surface finish quality and presence of defects are consistent with the outcome of the mechanical characterization tests and the results of previous literature studies concerning FFF 3D printing processes; in fact, it is well known that the presence of porosity in plastic components triggers the generation of cavities and micro cracks, causing large deformations and increasing the ε_f. Likewise, the strength and the elastic modulus of the parts decrease as the number of defects increases [30–32]. This is in line with the results shown in Fig. 6.

The decrease in mechanical properties and the arising of defects could also be related to the increase in the nozzle diameter D_o without a corresponding increase in material flow rate. In fact, the use of a bigger nominal diameter nozzle could even bring benefits such as an increase in mechanical properties and a reduction of the printing time [33]; however, the flow rate should be adjusted accordingly to the nozzle wear in order to avoid the mechanical properties loss registered in this study. A comprehensive study on flow rate in relation with the nozzle wear and its progressive adjustment could results in an increase in service lifetime of the tools and, consequently, a reduction in parts costs and environmental impacts. In addition to the material flow rate, an investigation into the wear of nozzles used in FFF processes also could involves studying the process temperature at which the nozzle operates and how it may influence wear and wear rate. These themes are left as future work of this study.

4 Conclusions and further developments

In the present paper, the nozzle wear during FFF process was investigated and correlated to the mechanical properties of 3D printed parts in composite material. A polyamide filament reinforced with carbon fibers (Carbon PA) was selected as raw material, due to the high abrasion effect of the short fibers on the nozzle. The time dependence of the nozzle wear was investigated by interrupting the FFF process at fixed time intervals. Tensile specimens were produced to analyze the effect of nozzle wear on the mechanical properties of printed parts. Performance indicators, such as tensile strength, strain to failure, and elastic modulus, were assessed and plotted as a function of the nozzle service life. Optical microscopy investigation and X-ray computed tomography were used to monitor the external and internal nozzle wear evolution. The surface quality of the 3D printed parts was evaluated by means of surface roughness tester. Furthermore, the scanning electron microscopy was used to observe the three-dimensional topography of the longitudinal sections of filament in Carbon PA, at different printing time values, and fractured surfaces of tensile samples. Finally, the different surface finish obtained and the presence of voids and macro-defects in the specimens were correlated to the different nozzle wear level during the additive manufacturing process. The main results of the study can be summarized as follows:

- The mechanical properties of 3D printed parts are significantly affected by the printing time, which is related to the nozzle wear level occurred during the FFF process; specifically, a decrease both in mechanical strength and elastic modulus and an increase in strain to failure can be obtained with rising printing time.
- The wear is particularly enhanced on the external surfaces of the nozzle, where the increase in the bore chamfered and the drastic edge rounding of the external diameter of the nozzle appear, caused by the abrasion phenomena at the contact between tool and deposited extruded material.
- No appreciable internal nozzle wear appears; only the presence of material adhered to the inner surface of nozzle was confirmed by the reduction in section of the extruded filament using the worn nozzle as compared to the mean value in diameter of the extruded filament obtained using the wear-free nozzle.
- The nozzle wear, leading to nozzle geometric changes, causes a worsening in the surface finish quality of the printed parts and the occurrence of voids and macro-defects inside the components.
- The fracture mechanism of the 3D printed parts at different printing time is consistent with the time dependence of the nozzle wear; specimens, obtained using the nozzle at its initial service life, exhibit a fracture surface characterized by a matrix yielding and matrix and fibers debonding, while the fracture of samples printed using the worn nozzle can be attributed to the many voids and intra-layers macro defects caused by the non-uniform and non-homogeneous filaments deposited by the worn nozzle, leading to a marked reduction in tensile strength of 3D printed part.

This work represents the first systematic study on nozzle wear for FFF 3D printing and its correlation with the mechanical performances of the produced parts. It has considerable industrial repercussions as it helps a correct choice of the process and the tools to be used to guarantee compliance with the design requirements. Given the importance of the problem of tool wear, this study can be widened to include different kind of nozzle and filament materials to create models to predict the service life of 3D printing tools. Moreover, the influence of different process parameters (e.g., printing speed) on the tool wear could be investigated in detail. These studies will enable to reduce wear phenomena and to extend the service life of the tools, resulting in significant industrial advantages.

Supplementary Information The online version contains supplementary material available at https://doi.org/10.1007/s00170-024-13035-7.

Acknowledgements The Grant of Excellence Departments, MIUR-Italy (ARTICOLO 1, COMMI 314-337 LEGGE 232/2016) MARLIC is gratefully acknowledged. The authors would also like to thank Prof. Manuela Cortese and Dr. Genny Pastore of the Marche Applied Research Laboratory for Innovative Composites (MARLIC), the platform of the Marche Region (Italy) in the context of "Sustainable manufacturing: eco-sustainability of products and processes for new materials and de-manufacturing."

Author contribution IB: software, writing, and formal analysis. TM: methodology, investigation, and visualization. CM: writing—reviewing and editing and investigation. MS: supervision, data curation, writing, and reviewing. All authors read and approved the final version of the manuscript.

Funding Open access funding provided by Università Politecnica delle Marche within the CRUI-CARE Agreement.

Declarations

Competing interests The authors declare no competing interests.

References

1. Segovia Ramírez I, García Márquez FP, Papaelias M (2023) Review on additive manufacturing and non-destructive testing. J Manuf Syst 66:260–286
2. Pradeepkumar Samgeetha S, Maharaj N, Prakash Sharma B (2023) Modelling of the design process challenges in additive manufacturing using PROMETHEE. Mater Today Proc 78:620–626. https://doi.org/10.1016/J.MATPR.2022.11.480
3. Gibson I, Rosen D, Stucker B, Khorasani M (2021) Design for additive manufacturing. Addit Manuf Technol:555–607. https://doi.org/10.1007/978-3-030-56127-7_19
4. Bianchi I, Forcellese A, Gentili S et al (2022) Comparison between the mechanical properties and environmental impacts of 3D printed synthetic and bio-based composites. In: Procedia CIRP. Elsevier, pp 380–385
5. Gardner L (2023) Metal additive manufacturing in structural engineering – review, advances, opportunities and outlook. Structures 47:2178–2193. https://doi.org/10.1016/J.ISTRUC.2022.12.039
6. Ni J, Ling H, Zhang S et al (2019) Three-dimensional printing of metals for biomedical applications. Mater Today Bio 3:100024. https://doi.org/10.1016/J.MTBIO.2019.100024
7. Ebrahimi A (2015) Application of additive manufacturing in marine industry. Int J Marine Sci Environ 5:87–92
8. Frketic J, Dickens T, Ramakrishnan S (2017) Automated manufacturing and processing of fiber-reinforced polymer (FRP) composites: an additive review of contemporary and modern techniques for advanced materials manufacturing. Addit Manuf 14:69–86
9. Madhavadas V, Srivastava D, Chadha U et al (2022) A review on metal additive manufacturing for intricately shaped aerospace components. CIRP J Manuf Sci Technol 39:18–36. https://doi.org/10.1016/J.CIRPJ.2022.07.005
10. Forcellese A, Simoncini M, Vita A, Di Pompeo V (2020) 3D printing and testing of composite isogrid structures. Int J Adv Manuf Technol 109:1881–1893. https://doi.org/10.1007/s00170-020-05770-4
11. Sharma A, Chhabra D, Sahdev R et al (2022) Investigation of wear rate of FDM printed TPU, ASA and multi-material parts using heuristic GANN tool. Mater Today Proc 63:559–565. https://doi.org/10.1016/J.MATPR.2022.04.015
12. Srinivasan R, Aravindkumar N, Aravind Krishna S et al (2020) Influence of fused deposition modelling process parameters on wear strength of carbon fibre PLA. Mater Today Proc 27:1794–1800. https://doi.org/10.1016/J.MATPR.2020.03.738
13. Sood AK, Equbal A, Toppo V et al (2012) An investigation on sliding wear of FDM built parts. CIRP J Manuf Sci Technol 5:48–54. https://doi.org/10.1016/J.CIRPJ.2011.08.003
14. Patel R, Desai C, Kushwah S, Mangrola MH (2022) A review article on FDM process parameters in 3D printing for composite materials. Mater Today Proc 60:2162–2166. https://doi.org/10.1016/J.MATPR.2022.02.385
15. Sahoo S, Sutar H, Senapati P et al (2023) Experimental investigation and optimization of the FDM process using PLA. Mater Today Proc 74:843–847. https://doi.org/10.1016/J.MATPR.2022.11.208
16. Cao D (2023) Enhanced buckling strength of the thin-walled continuous carbon fiber–reinforced thermoplastic composite through dual coaxial nozzles material extrusion process. Int J Adv Manuf Technol 128:1305–1315. https://doi.org/10.1007/s00170-023-12014-8
17. Cao D (2023) Fusion joining of thermoplastic composites with a carbon fabric heating element modified by multiwalled carbon nanotube sheets. Int J Adv Manuf Technol 128:4443–4453. https://doi.org/10.1007/s00170-023-12202-6
18. Cao D, Bouzolin D, Lu H, Griffith DT (2023) Bending and shear improvements in 3D-printed core sandwich composites through modification of resin uptake in the skin/core interphase region. Compos B Eng 264. https://doi.org/10.1016/j.compositesb.2023.110912
19. Liang X, Zhang C, Wang C et al (2023) Tool wear mechanisms and surface quality assessment during micro-milling of high entropy alloy FeCoNiCrAlx. Tribol Int 178:108053. https://doi.org/10.1016/J.TRIBOINT.2022.108053
20. Marousi M, Rimpault X, Turenne S, Balazinski M (2023) Initial tool wear and process monitoring during titanium metal matrix composite machining (TiMMC). J Manuf Process 86:208–220. https://doi.org/10.1016/J.JMAPRO.2022.12.047
21. Zabala B, Fernandez X, Rodriguez JC et al (2019) Mechanism-based wear models for plastic injection moulds. Wear 440–441:203105. https://doi.org/10.1016/J.WEAR.2019.203105
22. Bergstrom J, Thuvander F, Devos P, Boher C (2001) Wear of die materials in full scale plastic injection moulding of glass fibre reinforced polycarbonate. Wear 251:1511–1521. https://doi.org/10.1016/S0043-1648(01)00787-6
23. Olsson A, Hellsing MS, Rennie AR (2017) New possibilities using additive manufacturing with materials that are difficult to process and with complex structures. Phys Scr 92:053002. https://doi.org/10.1088/1402-4896/AA694E
24. Bianchi I, Forcellese A, Mancia T et al (2022) Process parameters effect on environmental sustainability of composites FFF technology. Mater Manuf Process 37:591–601. https://doi.org/10.1080/10426914.2022.2049300
25. Calignano F, Lorusso M, Roppolo I, Minetola P (2020) Investigation of the mechanical properties of a carbon fibre-reinforced nylon filament for 3D printing. Machines 8(3):52. https://doi.org/10.3390/MACHINES8030052
26. Peng X, Zhang M, Guo Z et al (2020) Investigation of processing parameters on tensile performance for FDM-printed carbon fiber reinforced polyamide 6 composites. Compos Commun 22:100478. https://doi.org/10.1016/J.COCO.2020.100478
27. Deshmukh SP, Shrivastava R, Thakar CM (2022) Machining of composite materials through advance machining process. Mater Today Proc 52:1078–1081. https://doi.org/10.1016/J.MATPR.2021.10.495
28. Pinto D (2017) Effect of tool wear & machinability studies on polymer composites; a review. Int J Eng Inf Syst (IJEAIS) 1:71–77
29. Di Pompeo V, Forcellese A, Mancia T et al (2021) Effect of geometric parameters and moisture content on the mechanical performances of 3D-printed isogrid structures in short carbon fiber-reinforced polyamide. J Mater Eng Perform 30:5100–5107. https://doi.org/10.1007/s11665-021-05659-7
30. Wang X, Zhao L, Fuh JYH, Lee HP (2019) Effect of porosity on mechanical properties of 3D printed polymers: experiments and micromechanical modeling based on X-ray computed tomography analysis. 11(11):1154. https://doi.org/10.3390/POLYM11071154
31. Liao Y, Liu C, Coppola B et al (2019) Effect of porosity and crystallinity on 3D printed PLA properties. Polymers 11(11):1487. https://doi.org/10.3390/POLYM11091487
32. El AA, El M, Haddou Y, Khamlichi A (2016) Thermal-mechanical coupled manufacturing simulation in heterogeneous materials. Civil Eng J 2:600–606. https://doi.org/10.28991/CEJ-2016-00000062
33. Triyono J, Sukanto H, Saputra RM, Smaradhana DF (2020) The effect of nozzle hole diameter of 3D printing on porosity and

tensile strength parts using polylactic acid material. Open Eng 10:762–768. https://doi.org/10.1515/ENG-2020-0083